Biophysical Chemistry 148 (2010) 112–120

Contents lists available at ScienceDirect

Biophysical Chemistry

journal homepage: http://www.elsevier.com/locate/biophyschem

In vitro association of fragments of a β-sheet membrane protein

D. Debnath [a,b], K.L. Nielsen [b], D.E. Otzen [a,b,*]

[a] *Centre for Insoluble Protein Structures (inSPIN), Interdisciplinary Nanoscience Centre (iNANO), Department of Molecular Biology, University of Aarhus, Gustav Wieds Vej 10C, DK-8000 Aarhus C, Denmark*
[b] *Department of Life Sciences, Aalborg University, Sohngaardsholmsvej 49, DK-9000 Aalborg, Denmark*

ARTICLE INFO

Article history:
Received 20 January 2010
Received in revised form 9 March 2010
Accepted 10 March 2010
Available online 16 March 2010

Keywords:
OmpA
Cleavage sites
Association
SDS-PAGE
Proteolysis
Complementary fragments

ABSTRACT

Although the β-barrel membrane protein OmpA can be produced in a biologically active form in *E. coli* from co-expressed fragments, the fragments have not been demonstrated to associate *in vitro*. We have produced 3 complementary fragment pairs of OmpA which can associate to form a folded complex according to the SDS band-shift assay. We are able to convert 25–35% of the fragment populations to non-covalent but SDS-stable complexes. The periplasmic chaperone Skp effectively prevented this association. Two separately expressed and purified overlapping fragments of OmpA can form a protease-resistant complex that undergoes the characteristic band-shift upon heating. Our work demonstrates that although membrane insertion and folding of β-barrel membrane proteins may be a cooperative process, the fragments can associate *in vitro* without any additional components. However, the low yield and slow folding rates indicate that partially unfolded or destabilized β-sheet membrane proteins can potentially engage in many non-native interactions.

1. Introduction

Several models of folding of water-soluble proteins, such as the diffusion–collision model [1] and the extended nucleation condensation model [2], propose that folding begins at the local sequence level with structural elements that stabilize each other by associating, leading to native-like secondary structure and tertiary packing. The two models differ in the extent to which they emphasize the stability of the individual elements, which is considered to be significant in the diffusion–collision model and marginal in the extended nucleation condensation model. Support for both models can be found from studies of protein fragments. There is ample experimental evidence that peptide fragments (microdomains) with native-like folding propensity are able to interact with complementary fragments to form a native protein. For example, fragments of soluble proteins such as RNase A, Bovine Pancrease Trypsin Inhibitor [3], thioredoxin [4], Trp repressor [5], PRA-isomerase [6,7], chymotrypsin inhibitor 2 [8–10] and ubiquitin [11] can associate to form functionally active protein. In some cases, the fragments do not have persistent structure on their own and only fold stably when they dock to neighbouring domains [12,13], whereas in other cases individual fragments can have high levels of secondary structure [14].

Studies on the association of protein fragments provide valuable insight into the folding of intact proteins. This approach has also been used with membrane proteins. In this class of proteins, the low polarity and lack of hydrogen bonding partners amongst the acyl chains of the membrane hydrocarbon interior drive the protein or peptide to adopt structures that satisfy internal hydrogen bonding requirements [15–18]. For α-helical membrane proteins, where each α-helix is able to form internal hydrogen bonds, this effectively forces each helix to act like independent folding units. Individual transmembrane helices can generally form helical structures on their own [15,19], although some have higher propensities than others [20]. The latter aspect may reflect the vectorial folding pattern of α-helical membrane proteins where the later parts are added stepwise as they are transferred out from the translocon into the lipid phase and therefore do not need to have such high α-helix propensities [21]. Split α-helix membrane proteins also assemble *in vivo* when co-expressed, as shown for *e.g.* bacteriorhodopsin [22,23] and lactose permease [24].

The situation is different for β-barrel membrane proteins such as the outer membrane protein OmpA, given that hydrogen bonds are formed between residues far apart in the primary structure which need to come together. Indeed, pioneering studies by Kleinschmidt and Tamm indicate that OmpA folds by a concerted mechanism [25], in which formation of secondary and tertiary structure is synchronized [26], much like the nucleation–condensation mechanism of folding of water-soluble proteins [2]. The concerted nature of folding does not rule out that fragments of barrel-forming proteins can associate to form the native state. For example, the heptameric α-hemolysin from *S. aureus* forms a membrane-spanning β-barrel pore

Abbreviations: OM, octyl maltoside; TM OmpA, transmembrane part of outer membrane protein A.

* Corresponding author. Interdisciplinary Nanoscience Centre (iNANO), Department of Molecular Biology, Aarhus University, Gustav Wieds Vej 10C, 8000 Aarhus C, Denmark. Tel.: +45 89 42 50 46; fax: +45 86 12 31 78.
E-mail address: dao@inano.dk (D.E. Otzen).

0301-4622/$ – see front matter © 2010 Elsevier B.V. All rights reserved.
doi:10.1016/j.bpc.2010.03.004

containing one hairpin from each subunit [27], and there is evidence that most of the secondary structure is formed prior to assembly [28]. Furthermore, Wimley et al. have developed elegant schemes to select peptides which are unstructured in solution but assemble in the presence of membranes to form β-sheet rich pores [29], although it is not clear whether *bona fide* β-barrels are formed.

OmpA itself consists of 325 residues, of which residues 1–176 form an 8-stranded β-barrel in the outer membrane with 3 periplasmic turns and 4 surface-exposed loops [30], while the C-terminal domain extends as a globular domain into the periplasmic domain [31]. Seminal studies by Koebnik showed that fragments of OmpA could assemble *in vivo*, provided the polypeptide was split at the second or third (but not first) periplasmic turn of the transmembrane domain [32]. In addition to complementary fragments, overlapping fragments of OmpA (with an overlap of β-strands 5–6) also formed a functional complex *in vivo* [32].

However, it is unclear to what extent fragment association is aided by periplasmic chaperones and whether they can occur spontaneously. We have therefore decided to address to what extent productive association of OmpA fragments can occur *in vitro*. OmpA is a very useful model system for these studies, given that the intact protein inserts spontaneously into synthetic phospholipid membranes [33] and surfactants [34] without the need for metabolic energy. We have therefore made constructs of the transmembrane N-terminal domain of OmpA with engineered protease cleavage sites in each of the three periplasmic turns, in order to produce complementary fragments whose association can be monitored by the formation of stable complexes on SDS-PAGE gels. OmpA is known to tolerate both insertion of peptides into periplasmic turns [35] and substantial shortening of surface-exposed loops [36]. To optimize folding efficiency, we refold the fragments in the presence of 50 mM of the surfactant octyl maltoside (OM, critical micelle concentration 20 mM) rather than phospholipid vesicles, as micelles generally lead to faster refolding than vesicles [26]. We find that equimolar concentrations of complementary fragments, as well as overlapping fragments, can indeed assemble to form heat-modifiable and protease-resistant complexes, although with relatively low (<30%) efficiency and at very slow rates compared to the intact protein. This highlights the intrinsic activation barriers facing folding of outer membrane proteins and emphasizes the cooperative nature of the folding step.

2. Materials and methods

2.1. Materials

Genenase I (hereafter referred to as genenase) and trypsin were from New England Biolabs (Beverly, MA). Urea, Gly, EDTA were from Sigma (St Louis, MO). Octyl maltoside (OM) was from Anatrace (Maumee, OH). All SDS-PAGE was carried out using a 15% polyacrylamide separation gel prepared according to Laemmli [37]. Plasmids pQE60 and pPLT13 were generously provided by Dr. Jörg Kleinschmidt.

2.2. Construction of engineered OmpA expression plasmids with genenase cleavage sites

The transmembrane domain of the OmpA gene (residues 1–176) was engineered to produce four constructs: wild type and three variants in which a genenase recognition site (sequence GAAHYALGQPNV) was inserted in periplasmic turn 1 (TM OmpA1), turn 2 (TM OmpA2) and turn 3 (TM OmpA3), respectively (see Table 1 for details). In addition, the sequence Arg-Ser-$(His)_6$ was inserted at the C-terminus. These constructs were made by overlap extension using the primers listed in Table 2 and two stages of 25 PCR cycles of 95 °C for 30 s, 55 °C for 30 s, and 72 °C for 2 min. First stage included a relevant mutagenesis primer combined with either 5′-forward or 3′-reverse generic OmpA primer and a full length OmpA cDNA clone as template, and the second stage relevant pairs of the amplified fragments from the first stage and 5′-forward and 3′-reverse primer, as described [38]. The resulting amplified DNA fragments were digested with EcoRI and BamHI and inserted into pET3a (Novagen). Following transformation into *E. coli* TOP10 strain and selection for ampicillin resistance, a clone for each construct was identified and verified by DNA sequencing.

Table 1
Amino acid sequence, genenase recognition site, molecular weight and fragment size of constructs used in this study.

Construct	Amino acid sequence[a]	Position of genenase cleavage site (GN[b]) within the β-strand sequence[c]	Calculated molecular weights (Da) [d]
Wt TM OmpA	Aa 1–176	No GN site	20,398
TM OmpA 1	Aa 1–44-GN-aa 45–176	β_{1-2}-GN-β_{3-8}	5196, 16,399
TM OmpA 2	Aa1–87-GN-aa 88–176	β_{1-4}-GN-β_{5-8}	9962, 11,632
TM OmpA 3	Aa 1–133-GN-aa 134–176	β_{1-6}-GN-β_{7-8}	14,949, 6646
F2	Aa 48–176 (β_{3-8})	No GN site	15,460
F3	Aa 1–88 (β_{1-4})	No GN site	10,805

[a] All sequences contain Met at the N-terminus and RSHHHHHH at the C-terminus.
[b] Genenase cleavage site (GN): GAAHYALGQPNV. Cleavage occurs between His and Tyr.
[c] Subscripts refer to β-strand numbers.
[d] For the three TM OmpA constructs with genenase cleavage sites, molecular weights refer to the two N- and C-terminal fragments, respectively, produced from cleavage by genenase.

2.3. Preparation of F2 and F3 fragments

These were prepared using the primers described in Table 2 using the same PCR and ligation strategy as for the OmpA engineered variants. The forward primers includes the restriction site for NdeI and the translation ATG codon. The reverse primer includes a $(His)_6$ tail, two codons for translational stop and the restriction site for BamHI.

2.4. Purification of Skp and FkpA

Skp was purified as described [39] using plasmids pQE60 and pPLT13. The gene for FkpA was PCR amplified from the *E. coli* genome using the primers listed in Table 2 and cloned into a pET3a vector using restriction enzymes NedI and HindIII. After expression, cells were pelleted and resuspended in a cold solution of 50 mM Tris pH 8.0, 10 mM EDTA and 20% (w/v) sucrose before pelleting again. The supernatant was discarded and the pellet resuspended in water. MES pH 6.0 was added to 20 mM, and FkpA was purified on an SP-Sepharose column using a 0–500 mM NaCl gradient.

2.5. Expression and purification of TM OmpA constructs and F2 and F3 fragments

Plasmids were transformed into *E. coli* BL21 *plys*S or BL21 Gold. Protein was expressed and purified from the inclusion body fraction following standard protocols [33,40,41] with minor modifications. Instead of 50 μg/ml ampicillin, we used 100 μg/ml. For BL21 *plys S* host cell, we also included 25 μg/ml chloroamphenicol to retain the *plysS* plasmid. Protein was isolated from the inclusion body (IB) fraction. The IB fraction was incubated with TEN buffer (20 mM Tris pH 8.0, 1 mM EDTA, 100 mM NaCl) as well as 2% (w/v) Triton X-100 overnight at 37 °C, spun down and washed 2–3 times in 5 ml TEN buffer. Subsequently the pellet was dissolved in 4 ml TNU buffer, (20 mM Tris, 100 mM NaCl, pH 8.0 and 8 M urea) at 37 °C. All OmpA constructs except F2 were subsequently purified from the

Table 2
Design of primers used to prepare TM OmpA variants and other proteins used in this study. The genenase recognition sequence is included in the primer for TM OmpA 1–3.

Constructs	Forward primer	Reverse primer
Generic OmpA primers[a]	caccatggctccgaaagataacac	*ttatta*atggtgatggtgatggtgactacgagctgcttcgccctgaccg
TM OmpA 1[b]	ggcgcggcccattacgccctaggccagccgaacgtgtatgttggctttgaaatgg	cacgttcggctggcctagggcgtaatgggccgcgcccgggttaacctggtaacca
TM OmpA 2[b]	ccgggcgcggcccattacgccctaggccagccgaacgtggacgatctggacgtatacactc	cacgttcggctggcctagggcgtaatgggccgcgcccggagtgattgggtaacccagtttag
TM OmpA 3[b]	ccgggcgcggcccattacgccctaggccagccgaacgtggaaatcgctacccgtctg	cacgttcggctggcctagggcgtaatgggccgcgcccggaggagtgatcgcatactcaac
F2[a]	gggaattccatatgtatgttggctttgaaatgggttac	gcgggatcc*ttatta*atggtgatggtgatggtgactacgagctgcctcgccctgacc
F3[a]	gggaattccatatggctccgaaagataacacctg	gcgggatcc*ttatta*atggtgatggtgatggtgactacgagtgattgggtaacccagtttag
FkpA	gggaattccatatgaaatcactgtttaaagtaacg	ggcccaagctt*ttattat*tttttagcagaatctgcgg

[a] $(His)_6$ sequence underlined and stop codons in italics.
[b] Genenase recognition sequence underlined.

supernatant on a Ni^{+2} NTA column (Qiagen) using the manufacturer's instructions. The OmpA fractions were pooled and dialyzed overnight against a 50-fold volume excess of buffer D (20 mM Tris–HCl, 200 mM NaCl, 8 M urea, pH 8) to remove imidazole. After Ni-NTA purification, the intact OmpA constructs (OmpA TM 1–3) were refolded by dialyzing out urea very slowly with gradual (~20 ml/h) addition of a controlled volume of buffer containing 20 mM Tris, 2 mM EDTA, pH 10 to the dialysis solution bathing the dialysis bag. When the urea concentration had decreased to 3 M, 50 mM OM was added to the dialysate as well as the dialysis solution to prevent misfolding and aggregation. Fluorescence spectra of TM OmpA variants at 3 M urea showed that the protein remained soluble up to 4 mg/ml and unfolded, in good accord with Hong and Tamm [42]. Finally, when the urea concentration had decreased to 50–100 mM, the protein solution was dialyzed in fresh buffer including 50 mM OM. For samples subsequently used for genenase digestion, dialysis was halted at 3 M urea, and the sample was dialysed with genenase digestion buffer (100 mM NaCl, 50 mM Tris–HCl, 1 mM $CaCl_2$, pH 8.0) containing 3 M urea. F2 was dialyzed against 20 mM Tris pH 9.0 and 8 M urea before being loaded at 0.5 ml/min onto a 2 ml Q-Sepharose column (Amersham Biosciences, Uppsala, Sverige). The protein is eluted with a 0–1 M NaCl gradient and F2 fragments are identified by SDS-PAGE.

2.6. Genenase cleavage

Each of the OmpA constructs was digested with genenase to generate two fragments. Genenase is a variant of subtilisin BPN′ that has been engineered to cleave specifically after His in the sequence Pro-Gly-Ala-Ala-His-Tyr [43,44]. We digested OmpA in the unfolded state (in 3 M urea) at 28 °C in 20 mM Tris–HCl,200 mM NaCl, pH 8.0. Genenase cleaves nonspecifically at 37 °C, leading to complete digestion. 5 µg genenase was added to 350 µg of OmpA in a final volume of 100 µl. The solution was incubated for 18–20 h, and the extent of cleavage was monitored using 15% SDS-PAGE. After complete cleavage of protein, genenase was inactivated by adding 10 µl of complete protease inhibitor cocktail from Roche and the cleavage mixture was stored at −20 °C. Subsequent association experiments were carried out in the presence of 2 mM EDTA at 4 °C to ensure essentially complete absence of genenase activity (incubation at higher temperatures led to degradation of fragments).

2.7. Folding kinetics of intact OmpA constructs

The folding/unfolding kinetics of TM OmpA constructs in OM micelles were monitored via SDS-PAGE as the folded and unfolded states migrate differently (with apparent molecular weights of 21 and 23 kDa, respectively) [33]. Typically, protein was diluted directly from 8 M urea to the refolding buffer containing 20 mM Gly, 2 mM EDTA, 50 mM OM pH 10, giving a residual urea concentration of 270 mM. All folding kinetics of intact OmpA constructs were conducted at 25 °C At different time points, 30 µl of reaction mixture was immediately mixed with 10 µl 4× sample buffer (without reducing agents) to arrest folding and subsequently analyzed by SDS-PAGE without prior boiling (unless otherwise stated). The amount of folded and unfolded protein was quantified by scanning densitometry using a conventional scanner in combination with the programme ImageJ. Band intensities were and subsequently fitted to a double exponential decay:

$$y = A_1 * \exp\left(-x * \ln(2) / t_1\right) + A_2 * \exp\left(-x * \ln(2) / t_2\right) + c \qquad (1)$$

where A_1 and A_2 are amplitudes, t_1 and t_2 are half lives and c is the offset. Fitting was done using the programme Kaleidagraph 4.0 (Synergy Software).

2.8. Association of TM OmpA fragments

100 µl of digested OmpA (~300 µg) in 3 M urea was diluted out to a final volume of 750 µl in different (30, 50 and 100 mM) concentrations of OM and 20 mM Gly, 2 mM EDTA, pH 10.0 and a residual urea concentration of 400 mM urea. These conditions are those used for typical full length OmpA refolding experiments, where the high pH reduces the degree of aggregation in the denatured state [34]. All fragment association experiments were conducted at 4 °C. At different time points, 15 µl were taken out, immediately mixed with 5 µl 4× sample buffer and subjected to SDS-PAGE. Associated TM OmpA fragments migrate as a band of ~23 kDa. The band intensity was quantitated by scanning as above. Genenase also produced some smaller fragments to a small extent. However, to simplify the analysis we restricted the densitometry analysis to the bands corresponding to the 2 fragments and the complex. The fraction of assembled fragments was plotted as function of time and fitted to a double exponential decay (Eq. (1)) or to a single exponential decay in which the second term in Eq. (1) was removed.

Trypsin digestion was performed by mixing 0.2–2% trypsin (w:w) with 35 µg of total TM OmpA1 (fragments and complex) for 20 min at room temperature in 20 mM Tris, 2 mM EDTA, pH 8.0, before mixing with the required amount of 4× sample buffer and carrying out SDS-PAGE.

2.9. Trypsin digestion and mass spectrometry

15 µM OmpA fragments (F2, F3 and F2:F3) in 10 mM borate buffer pH 8 and 50 mM octyl maltoside were incubated at 37 °C for 12–16 h. 6.25 µl of 2 mg/ml trypsin was added to the sample followed by 30 minute incubation on ice. $CaCl_2$ was added to 90 mM, after which the sample was incubated for 30 min at 37 °C. Proteolysis was halted by adding 0.33 mg/ml soy bean trypsin inhibitor, incubating 15 min on ice and mixed 1:1 with SDS sample loading buffer. After running the samples on SDS-PAGE, the appropriate bands were cut out, incubated for 20 min in 400 µL 50 mM Tris (pH 8,59) and excess liquid removed by centrifugation. This was carried out 3 times, after which the band was mixed with 100 µl 5 µg/ml trypsin solution and incubated for 10 min on ice. Excess trypsin buffer was removed and the band was covered with 50–100 µl digestion buffer (10 mM Tris, pH 8) and left at 28 °C for 12–16 h. Proteolysis was stopped by adding

5 µl 10% acetic acid, and the supernatant was subsequently transferred to an Eppendorf tube containing 10 µl R2 spheres (Applied Biosystems, USA) onto which the peptides could bind and subsequently be eluted. The trypsin-digested peptides were washed with 100 µl aliquots of 10% acetic acid (twice), deionized water, 25% acetonitrile and deionized water. After each step, the R2 tube was centrifuged and the supernatant removed. Finally, the peptides were eluted by adding 3 µl 25% acetonitrile and 0.1% trifluoroacetic acid, incubating for 5 min, and centrifuging for 5 min. 1 µl of the supernatant from this solution was mixed with 1 µl DHB matrix, transferred to the anchor chip plate and analyzed by MALDI-TOF MS (Bruker Daltronics Reflex III).

3. Results

3.1. Incorporation of genenase sequence does not impair folding of OmpA although it slightly alters folding kinetics

To prepare fragments of OmpA for association studies, we introduced genenase cleavage sites into the 3 periplasmic turns of OmpA. Modification of these periplasmic turns by the insertion of 8 extra residues could affect the topological properties of OmpA, since the wt periplasmic turns constitute tight β-turns which will be relaxed by the turn expansion. At the same time, the behaviour of the OmpA constructs in which these turns are replaced will itself provide information on the role of these turns in folding. We found that all 3 variants were able to fold according to the usual criteria for folding of outer membrane proteins. Firstly, they all showed the expected SDS-PAGE band-shift from the denatured to the native state over time when allowed to refold from 8 M urea into 50 mM octyl maltoside (OM) and residual (270 mM) urea (Fig. 1A). Secondly, all 3 variants underwent a characteristic blue shift in the fluorescence emission spectrum from 354 nm in 8 M urea to 335 nm in the presence of 50 mM maltoside at low urea concentrations (data not shown). Wt TM OmpA undergoes a similar blue shift in DOPC vesicles [25] and in OM. These data confirm that introduction of the Genenase cleavage sites does not prevent proper folding of OmpA.

Nevertheless, the kinetics of folding could still be affected. Therefore we followed the OmpA refolding time course by diluting the protein from 8 M urea into 270 mM urea and 50 mM OM. At different time points, samples were removed and transferred to SDS-PAGE loading buffer to halt the folding reaction, after which the sample was analyzed by SDS-PAGE (Fig. 1A) and band intensities were plotted versus time (Fig. 1B). As summarized in Table 3, each of the constructs showed a biphasic folding profile, involving a fast as well as a slow refolding phase. Since our SDS-PAGE method directly monitors the formation of the native state (rather than a spectroscopic intermediate), this suggests that there are parallel folding pathways, as reported previously by Kleinschmidt and Tamm [25]. The refolding kinetics of TM OmpA1 (where the cleavage site is inserted into the first periplasmic turn) are essentially unchanged compared to wt OmpA, whereas significant changes are observed for both TM OmpA2 and TM OmpA3. The fast phase is slowed down by an order of magnitude for these mutants; in addition the slow phase has become the dominant phase for TM OmpA2, taking up 64% of the total amplitude (in contrast to 10–20% for the other three constructs). Thus folding kinetics are strongly affected by changes to periplasmic turns 2 and 3 but not in turn 1. Interestingly, the largest effect is seen in the most central insertion (turn 2).

3.2. A significant fraction of the OmpA fragment population can associate to form complexes, though the kinetics vary for different fragment pairs

Having established that the inserted cleavage site does not prevent proper refolding, we then prepared the individual fragments. Each of the TM OmpA variants was split in two parts by cleavage with genenase in the presence of 3 M urea. This denaturant concentration was a compromise between two opposing requirements: high denaturant concentrations allow us to keep the fragments soluble and provide access to the cleavage site, while low concentrations are required to retain protease activity. Cleavage at lower urea concentrations and in the presence of OM did not destabilize the protein sufficiently to allow access for genenase (data not shown).

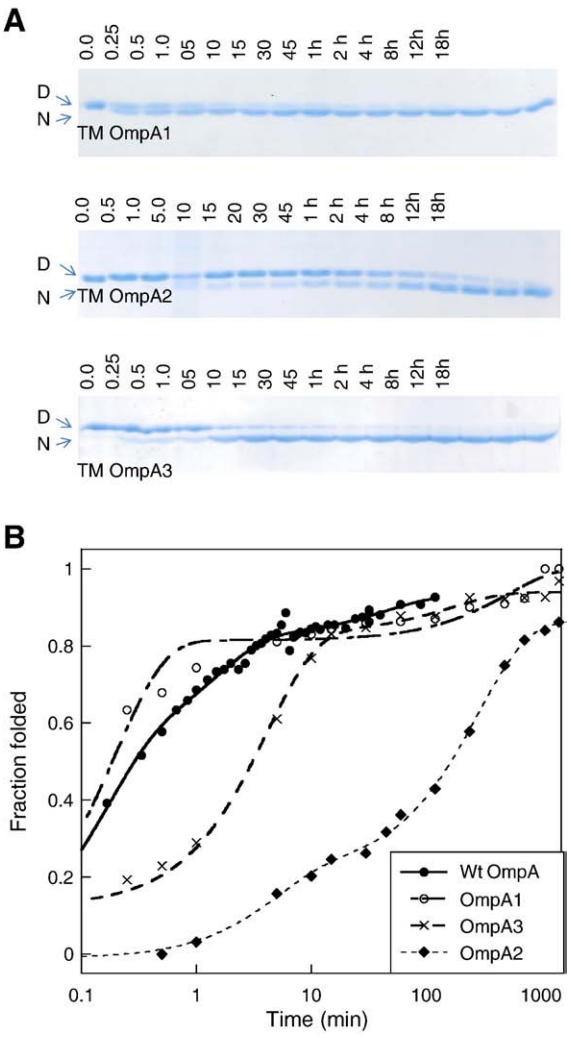

Fig. 1. (A) Refolding of the three TM OmpA constructs in 50 mM octyl maltoside (OM) monitored by SDS-PAGE and followed over time. All experiments in 20 mM Gly, 2 mM EDTA pH 10, 50 mM octyl maltoside at 25 °C. (B) Plot of the fraction folded vs time of the three OmpA constructs as well as wt OmpA. Errors on each measurement point ca. 5%. Data fitted to double exponential decays and summarized in Table 3. Note the logarithmic time scale which makes it easier to distinguish the data from the individual constructs.

Table 3
Band-shift monitored folding of intact OmpA constructs[a,b].

	Amp1	$t^1_{½}$ (min)	Amp2	$t^1_{½}$ (min)
Wt OmpA	81.2 ± 3.1	0.11 ± 0.01	18.8 ± 2.5	170 ± 60
TM OmpA1	81 ± 4	0.14 ± 0.02	19 ± 1	360 ± 280
TM OmpA2	23 ± 1	3.3 ± 0.5	65 ± 1	200 ± 10
TM OmpA3	70 ± 3	2.8 ± 0.4	11 ± 3	110 ± 80

[a] All experiments in 20 mM Gly, 2 mM EDTA pH 10, 50 mM octyl maltoside and residual urea (0.4 M).
[b] Kinetic parameters obtained from fitting band intensities in Fig. 1B to a double exponential decay (Eq. (1)), giving the amplitudes (Amp) and half lives ($t_{½}$) for each of the two phases.

Cleavage of TM OmpA1 and TM OmpA3 produces two fragments, each of molecular weights ~16 and ~6 kDa while cleavage of TM OmpA2 produces two fragments of very similar size (11.5 and 10.2 kDa) (Table 1 and Fig. 2). For TM OmpA1 and TM OmpA2, we observe a small amount (≤10%) of unspecific cleavage, depending on the genenase batch used (data not shown). The unspecific cleavage was more pronounced for TM OmpA3, where a smaller band was consistently observed below the two expected bands (see asterisk in Fig. 2). However, these bands were not included in the subsequent densitometric analysis, which only involved the 2 correctly sized fragments and the non-covalent complex formed by their association. In accordance with their origin as equimolar cleavage products from a single precursor protein, the two fragments show approximately equal band intensities.

Using SDS-PAGE, we are able to follow the association of the two fragments in the presence of OM through the formation of a band migrating at the same position as the folded uncleaved protein (23 kDa, Fig. 3A). In the case of TM OmpA1 we also saw a significantly fainter band migrating above the folded band at a position corresponding to unfolded OmpA (indicated with an asterisk in Fig. 3A). This band started to appear well after the folded band. The faintness of the band meant that it did not contribute significantly to the overall intensity of the complex bands and was therefore left out of our calculations. Trypsin-treatment of the sample made this band more fuzzy (data not shown). This suggested that it was possible for the two fragments β-strands 1–2 and β-strands 3–6 to associate to a partially folded (but protease-sensitive) complex, which was nevertheless stable enough to (at least partially) withstand dissociation in SDS.

The associated complex was a well-defined species which unlike the individual fragments was resistant to protease treatment (see also below for further details) and is dissociated by heat treatment (data not shown).

We quantified the rate of appearance of the folded TM OmpA complexes in the presence of 50 mM OM from the increase in intensity of the complex band (Fig. 3B). The association kinetics varied significantly among the 3 complexes. Association of TM OmpA1 fragments follows biphasic kinetics, with a fast phase showing a $t_{½}$ around 7.1 min and a slow phase with a $t_{½}$ around 650 min (Table 4). In contrast, association of the two other fragments followed single exponential kinetics. Just as for the intact variants, association of TM OmpA2 fragments is significantly slower than that of the two other fragments.

To complement our association data, we also monitored the parallel decrease in intensity of the fragments (Fig. 4A). The half lives of this decrease agree reasonably with the association kinetics (Table 4), indicating that we are essentially monitoring the formation of a folded complex from the individual fragments. The fact that the two sets of half lives do not correspond exactly to each other may reflect that the fragments can be engaged in interactions other than the formation of native complexes. Importantly, we observe the same distinction between single exponential (TM OmpA2 and TM OmpA3) and double exponential decay (TM OmpA1).

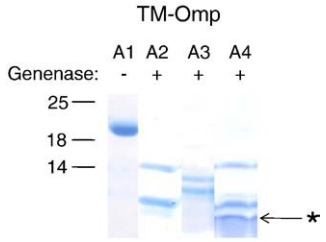

Fig. 2. Digestion of TM OmpA1–3 by genenase in 3 M urea. See Table 1 for calculated molecular weights of the fragments. Asterisk indicates unexpected cleavage product of TM OmpA3.

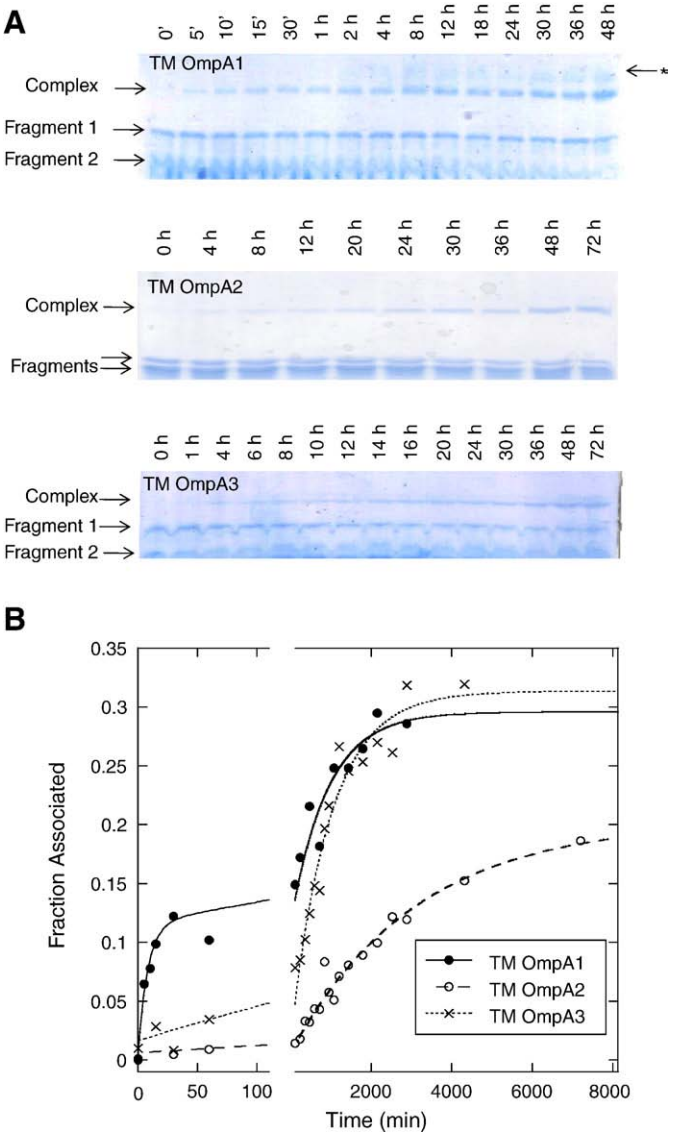

Fig. 3. Kinetics of association of the TM OmpA fragments in 50 mM OM. All experiments in 20 mM Gly, 2 mM EDTA pH 10, 50 mM octyl maltoside at 4 °C. (A) Association monitored by SDS-PAGE. Asterisk for TM OmpA1 denotes putative partially denatured complex. (B) Band intensities from panel A. Data for TM OmpA1 are fitted to a double exponential decay, while data for TM OmpA2 and TM OmpA3 are fitted to a single exponential decay. Errors determined from triplicate measurements. Data are summarized in Table 4.

Table 4
Kinetic parameters for the association of complementary OmpA fragments[a].

Mutant	Amp1	$t^1_{½}$ (min)	Amp2	$t^2_{½}$ (min)
TM OmpA1	10 ± 2%	7.1 ± 3.4	18 ± 2%	650 ± 220
Disappearance of β3–8	5.7 ± 0.9%	24 ± 12	18.9 ± 1.5%	1610 ± 200
TM OmpA1^{7M} [b]	9.6 ± 0.5%	21.7 ± 2.4	6.7 ± 0.6%	940 ± 260
TM OmpA2	–	–	20.0 ± 1.4%	2150 ± 310
Disappearance of β1–4 and β5–8	–	–	43 ± 2%	760 ± 140
TM OmpA3	–	–	29.1 ± 2.2%	715 ± 150
Disappearance of β1–6	–	–	30.2 ± 1.5%	670 ± 90

[a] All data based on reassociation of fragments upon dilution of an equimolar mixture of fragments from 3 M urea into 0.27 M urea, except data in row 3. All experiments in 20 mM Gly, 2 mM EDTA pH 10, 50 mM octyl maltoside at 4 °C. Kinetic parameters obtained by fitting band intensities (Figs. 3 and 4) to double or single exponential decays.

[b] Diluted from 7 M urea into 0.4 M urea.

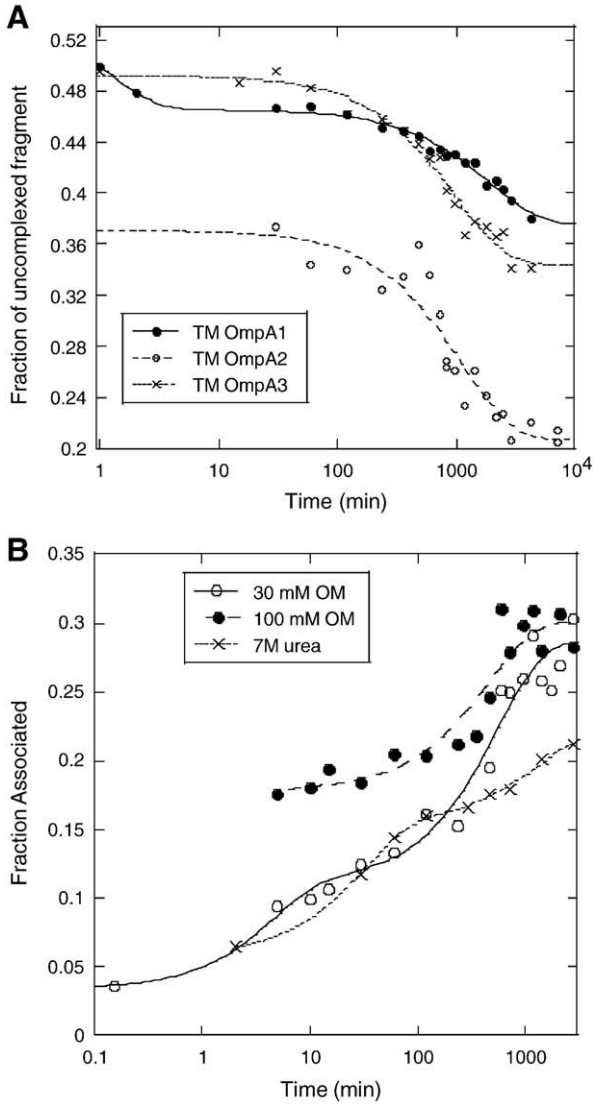

Fig. 4. A. The kinetics of disappearance of the larger fragments in TM OmpA1–3 in 50 mM OM monitored by SDS-PAGE. B. TM OmpA1 association in different concentrations of OM and starting from 7 M urea. Data are summarized in Table 4.

Note that in all cases only a fraction (25–30%) of the complexes associated, according to the intensity of the band of the associated complex compared to the total band intensity. Incubation of the fragments for up to 120 h did not increase the level of association beyond 30% (data not shown). The incomplete degree of association did not appear to be associated with higher-order structures. Apart from the partially folded putative complex mentioned above, we did not observe any higher-order bands which could be digested by trypsin (data not shown). Furthermore, changing the OM concentration from 50 to 30 or 100 mM OM did not significantly alter the association yield (Fig. 4B).

3.3. Residual structure prior to association

For practical purposes, OmpA was cleaved in 3 M urea in the absence of OM and the two complex fragments were associated by dilution from this urea concentration. It is possible that the fragments retain residual structure even at 3 M urea, which could influence the association reaction. Any such residual structure is likely to disappear at higher denaturation concentrations. When we transferred the OmpA1 fragment mixture to 7 M urea and incubated them for 1 h before reconstituting them by diluting out as before, we saw essentially the same folding half lives as when refolding from 3 M urea (Fig. 4B and Table 4). The fast reaction showed a half life of 21.7 min whereas the slow reaction had a half life of 941 min (Table 4) which lie within the same range as the formation of OmpA1 complex from 3 M urea as well as the disappearance of the β3–8 fragment. The only difference was that the amplitude of the slow phase had decreased by ~50% (Fig. 4B). This suggests that residual structure in the denatured state does not play a major role for the kinetics of fragment association, although it may have an impact on the amount of constructive association.

3.4. Skp inhibits fragment association

The periplasmic chaperone protein Skp is able to bind to unfolded OmpA and prevent its folding into phospholipid membranes [39,45]. Commensurate with this, when Skp is present during the fragment association of OmpA2 fragments at 1:1 weight ratio, it completely inhibits their association (Fig. 5). In contrast, the periplasmic chaperone FkpA, which has not been reported to be involved in the folding of OmpA [46], was unable to inhibit association (data not shown).

3.5. Specificity of fragment association

Given that we were able to induce association of complementary fragments, we tested whether other fragment combinations would also yield SDS-robust complexes. We therefore mixed all fragments of OmpA1, OmpA2 and OmpA3 generated from 3 separate Genenase cleavage reactions in an equimolar ratio, and reconstituted the fragment mixture by diluting from 3 M urea into 50 mM OM. We observe a band corresponding to the native state of OmpA (Fig. 6A), in addition to a 25 kDa band. This band corresponds in mobility to the partially unfolded state (cfr. Fig. 4B). Just as seen for association of TM OmpA1 fragments alone, the 25 kDa band accumulates more slowly than the appearance of the folded TM OmpA band and the disappearance of the large fragment band, probably β_{3-8} (Fig. 6B). In view of this, the 25 kDa fragment is unlikely to represent a hybrid complex between overlapping fragments. We can also safely exclude the formation of a complex between the two longest two fragments (β_{1-6} and β_{3-8}), which will give a molecular weight of ~31 kDa, which clearly is not visible on the gel.

Thus, even in the presence of four other fragments with very similar binding sites, each fragment preferentially interacts with its own complementary fragment. However, the data prompted us to investigate whether it was possible for overlapping fragments to associate in the absence of competing complementary fragments.

3.6. Fragment pairs with overlapping sequences can also associate to form a complex where the sequence from the smaller fragment is cleaved off

We attempted to separate the individual fragments of OmpA in order to study the extent to which they could individually be folded beforehand and the effect of this on the subsequent association.

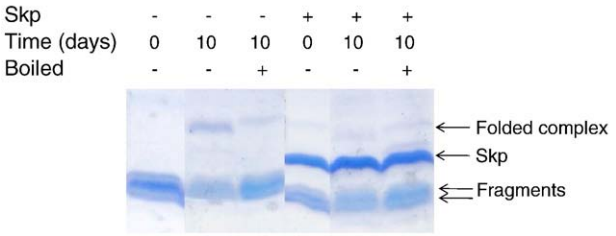

Fig. 5. Skp significantly reduces TM OmpA2 complexation monitored by SDS-PAGE. Skp is added at the same weight concentration as that of the combined weight concentration of the two OmpA fragments.

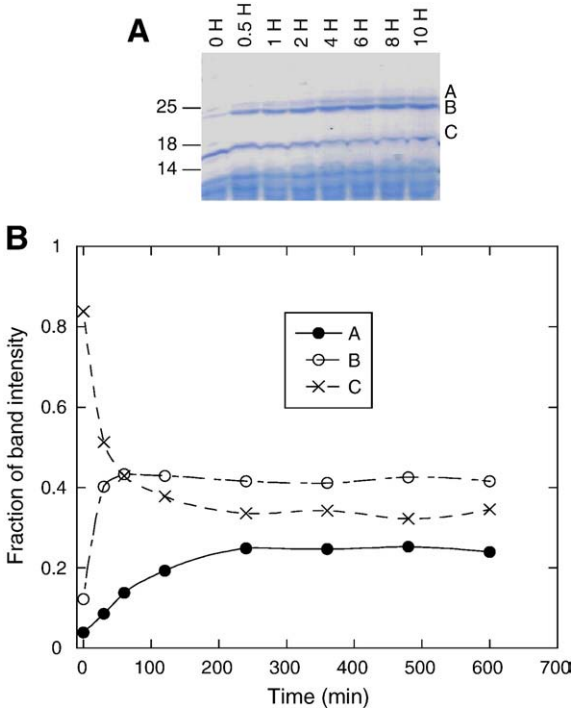

Fig. 6. (A) Digested TM OmpA1, TM OmpA2 and TM OmpA3 mixed together in equimolar amount and allowed to associate, as monitored by SDS-PAGE. All experiments in 20 mM Gly, 2 mM EDTA pH 10, 50 mM octyl maltoside at 4 °C. Band A corresponds to either a partially unfolded complex of complementary fragments or folded overlapping fragments, band B corresponds to the folded complex of complementary fragments and band C corresponds to the large fragments (β_{1-6} and β_{3-8}). (B) Band intensities of the 3 bands in panel A.

Unfortunately, we were unable to separate the fragments chromatographically. We also attempted to produce the individual fragments by separate expression of the sequences coding for each of the six sequences (without the Genenase cleavage site). However, despite repeated attempts, it was only possible to express and purify the overlapping fragments F2 (residues 48–176, corresponding to β-strands 3–8) and F3 (residues 1–88, *i.e.* β-strands 1–4) separately as inclusion bodies in *E. coli*. The other fragments failed to express to feasible levels (data not shown). We therefore used SDS-PAGE to investigate the extent to which these two fragments could associate.

As shown in Fig. 7A, F2 and F3 incubated at approximately equimolar concentrations are able to form a complex which dissociates upon heating. The association of F2 and F3 occurs with comparable yields over a wide pH range (pHs 4–8) (data not shown). Attempts to analyze the association of pre-folded fragments are complicated by the fact that F2 by itself is able to form an SDS-stable F2 dimer complex when diluted out into surfactant, although this is very faint, amounting to less than 5–10% of the entire population (data not shown). This ability to dimerize is analogous to the reported *in vivo* dimerization ability of the OmpA fragment β_{3-8} [32] and may partially explain the existence of excess free F3 in the complex mixture. In contrast, F3 upon dilution into surfactant typically forms visible aggregates which can only be dissociated upon transfer to 4 M urea.

The formation of a complex between two fragments with overlapping sequences immediately raises the intriguing question: which fragment's overlapping sequence is integrated into the complex and which sequence is displaced and remains unstructured? We addressed this issue by subjecting the complex to trypsin digestion under native conditions, reasoning that trypsin will only cleave off flexible regions of the complex. As shown in Fig. 7B, trypsin trims down the complex (as well as degrading most of the uncomplexed fragments), leaving behind a trypsin-resistant core.

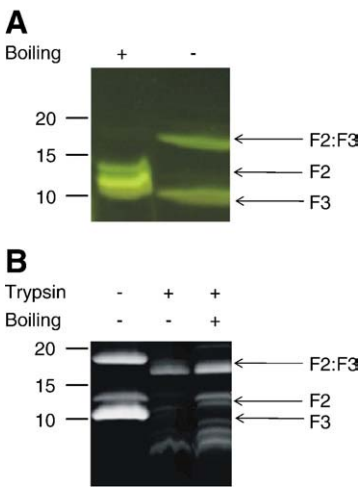

Fig. 7. (A) Association of overlapping F2 and F3 fragments in 20 mM Gly, 2 mM EDTA pH 10, 50 mM octyl maltoside at 4 °C. The complex dissociates upon boiling in SDS-PAGE sample buffer. (B) Trypsin digestion of the complex formed between overlapping F2 and F3 fragments. Note the small decrease in mass of the complex and the disappearance of most of the uncomplexed fragments.

When this complex is (partly) dissociated by boiling, we observe the original F2 and F3 fragments as well as what can be interpreted as a smaller fragment of F2 and two smaller fragments of F3 (Fig. 7B). Interestingly, the majority of F2 remains uncleaved whereas the opposite is the case for F3. This suggests that F2 is only partially trimmed to a small extent whereas F3 is trimmed to a great extent and the trimming occurs in at least two places. MS analysis (Table 5) nicely confirms this, identifying in the case of F3 only fragments corresponding to strands 1–2 (residues 1–64) as well as strands 1–3 (residues 1–73) whereas for F2, we observe both the entire fragment (residues 1–132, corresponding to strands 3–8) as well as a fragment with residues 19–132, corresponding to strands 4–8. Thus in all cases, the 4th β-strand comes from the larger F2 fragment whereas the 3rd strand may come from either F2 or F3. The topological model of the F2:F3 complex is summarized in Fig. 8.

4. Discussion

4.1. The second periplasmic turn appears to be central for fast folding

We have been able to monitor the association of complementary fragments of the transmembrane domain of OmpA through the insertion of a 12-residue protease cleavage site into each of the 3 periplasmic turns. We will first discuss the properties of the intact constructs. Previous work by Ried et al. established that the insertion of 4–12 extra residues in these turns did not interfere with OmpA assembly *in vivo*, although at least 12 residues were needed to allow trypsin to cleave these turns [35]. Nevertheless, it might be expected that the kinetics of assembly could be affected, given that the periplasmic turns are tightly constricted and only involve 4 residues in the wild type structure. Furthermore, the introduction of new termini in these loops by circular permutation of OmpA led to

Table 5
Summary of fragments from trypsin-digested F2:F3 complex identified by MS.

Fragment[a]	Measured Av mass [M + H]	Calculated Av mass [M + H]	Sequence
F3	7190.6 ± 2.1	7190.9	1Ala → 64Lys
F3	8096.7 ± 3.4	8096.9	1Ala → 73Lys
F2	12190.8 ± 10.5	12185.5	19Gly → 131Arg
F2	14523.2 ± 25.6	14498.3	1Met → 132Ser

[a] Full length F3 is 88 residues while full length F2 consists of 128 residues (Table 1).

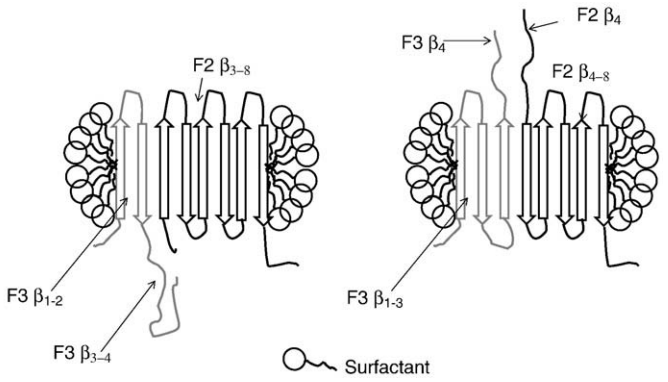

Fig. 8. Models of the two possible topologies of the complex formed by the overlapping fragments F3 (grey) and F2 (black), as suggested by the trypsin digestion pattern.

significant reductions in assembly yield and phage infectivity [47]. The greatest effects were seen upon altering the third turn (between β_6 and β_7), followed by the second turn (β_4 and β_5) and then the first turn (β_2 and β_3) [47].

Further insight can be provided from the folding kinetics *in vitro* of these constructs, since this will be very sensitive to changes in topological freedom induced by these insertions. Just for the circular permutants, the smallest change is effected by the insertion into the first turn, whose kinetics are essentially identical to that of wildtype OmpA (Table 3). However, unlike the circular permutants, we observe the greatest retardation of folding kinetics by the insertion into the second (central) turn, which skews the distribution between slow and fast phases so that the slow phase (which only accounts for ~20% of the folding population in wt TM OmpA) becomes the dominant species, although its folding kinetics are similar to those of wt TM OmpA. The fast phase is retarded by an order of magnitude in TM OmpA2 and TM OmpA3 compared to wt and TM OmpA1. Our data are consistent with the scenario that OmpA follows parallel folding pathways, in which the partitioning between the two pathways is determined by the topological accessibility of the two pathways. According to calculations using the prediction programme TANGO [48], the inserted protease cleavage sequence does not possess a high intrinsic β-turn propensity but does not appear to reduce the intrinsic β-turn propensities in the turn regions (calculations not shown). However, the extra loop formed at the turn region may affect the formation and stability of the β-hairpin involving the two β-strands around the turn. We speculate that entry into the fast track requires a well-defined second turn to avoid trapping OmpA in a more slowly folding state. This conclusion is corroborated by the fact that TM OmpA2 fragments (which completely lack the second turn) show a marked reduction in association kinetics compared to the two other fragment pairs (Fig. 2B). It seems plausible that interference with the central turn will have a greater impact on the topology than the two peripheral turns. Analogous conclusions have been drawn from loop-replacement studies of the 7-helical membrane protein bacteriorhodopsin, where mutations in the fourth and fifth inter-helical loops had the greatest impact on the rate-limiting folding step [49].

4.2. Low refolding yields may reflect trapping of TM OmpA in non-folded states

The most striking aspect of the association of complementary TM OmpA fragments is that folding is very slow and gives a very low yield (<30%) even under stoichiometric conditions. *In vivo* OmpA folds within 1–2 min [47], and the large majority of intact TM OmpA folds in a fast phase with half lives of a few minutes. The time scales are so long that the diffusion associated with complex formation will not be a limiting factor. Kinetics will naturally be slowed down due to the necessity of incubating at 4 °C, but this is only likely to affect kinetics by 2–3 fold. A clue to the low yield may come from the observation that refolding of fragments from 7 M urea (rather than the customary 3 M urea) leads to the same association half lives but a significantly lower yield. The OmpA fragments are unfolded and non-associated under both conditions (since our SDS-PAGE data show that association only starts upon dilution of the urea to sub-molar concentrations), but it is possible that there is a difference in the amount of residual structure present, which may affect the formation of different initial species formed upon dilution of the urea.

In the same way, the slow phase for the folding of intact OmpA may represent a slightly misfolded or collapsed state which has to rearrange itself to reach the native state, and that this type of slow folding phase has become the dominant feature in the association of TM OmpA fragments. A fast association phase is only observed for TM OmpA1, the only construct that shows wild type like folding behaviour in the intact state. The two other constructs show a retardation of the fast refolding phase and in the case of TM OmpA2 a dominance of the slow phase, indicating that they have an increased ability to pass through folding detours. Access to such misfolded states may be significantly easier for OmpA fragments, witness the ability of F2 to form (non-native) dimers and the tendency of F3 to form aggregates if diluted on its own.

Furthermore, Skp is able to recognize and bind to these fragments and halt the association process despite the presence of micelles, indicating that they are very easily trapped in the denatured state and only associate slowly and incompletely even in the presence of surfactants. This differs from the association of Skp with intact unfolded OmpA; Skp forms a stable complex with OmpA in the absence of membranes, but releases it when membranes are added [39].

It is likely that this tendency to form promiscuous and non-native interactions is an intrinsic feature among β-barrel proteins and may be unveiled by introducing destabilizing conditions where non-native interactions can occur. Even intact OmpA can be induced to form dimers and higher-order structures provided it is forced to fold under conditions where the amount of surfactant micelles is limiting (K.K. Andersen and D.E.O., unpublished observations). These dimers can exist both in the folded and partially unfolded state; in the latter case, the molecules must be held together by weak (but still SDS-resistant) non-covalent interactions. Similar conclusions about the promiscuity of β-sheet peptides in membrane environments have been reached by Wimley et al. [50], who observed that variants of a simple hexapeptide formed very similar β-sheets in a membrane environment. In a further testimony to the versatility of β-sheet interactions, the Lakey group was able to form asymmetric dimers of the trimeric porin OmpF [51]. While we cannot make any detailed predictions about the structures of these non-native states, it is possible that they include partially folded or molten-globule like structures where elements of fluctuating structure co-exist with some relatively stable β-strand structures engaged in intra- or inter-molecular interactions that prevent the formation of stable native interfaces.

4.3. Overlapping interactions illustrate versatility of β-sheet contacts

Koebnik reported that overlapping fragments of OmpA (the two fragments β_{1-6} and β_{5-8}, where β-strands 5 and 6 overlap) formed a folded and heat-modifiable complex [32]. He concluded from proteolytic studies on intact cells and spheroplasts (in which the orientation of the OmpA complex is constrained to direct the periplasmic loops inward) that this is caused by displacement of one β-strand from each fragment onto the outer membrane. When we use mass spectrometry to analyze a complex between two other overlapping fragments (β_{1-4} and β_{3-8}), we are also led to conclude that at least one of the two possible topologies involves displacement of one β-strand from each fragment (Fig. 8), though there is also good evidence for the scenario in which both strands of the longer fragment

are incorporated. This highlights the versatility of β-sheet contacts, as discussed in the previous section.

4.4. Implications for folding of β-barrel membrane proteins

Our data demonstrate that fragments of β-barrel membrane proteins are able to associate to form the folded state *in vitro*. Because of our inability to separate the individual fragments and the difficulty of expressing fragments separately, we are not able to make any clear conclusions about the degree to which the fragments can or must fold by themselves before productive association occurs. Nevertheless, the low level of productive folding indicates a pronounced tendency to engage in non-productive interactions. Such interactions could include intramolecular hydrogen bonding or intramolecular interactions which are stable enough to trap the fragments in non-native complexes but too weak to survive exposure to SDS and thus persist on SDS-PAGE. Such association behaviour is an intrinsic β-sheet property of interactions, which if unfettered can give rise to large self-assembled structures such as amyloid fibrils [52]. In contrast, it has been noted that the inter-helical contacts stabilizing the tertiary fold of α-helical membrane proteins typically involve van der Waals interactions mediated by "knobs into holes" contacts [15]. This provides a degree of specificity which reduces unwanted associations. Constructive folding of β-barrel proteins is promoted by retaining an intact protein and using chaperones such as Skp and lipids [39] to eliminate potential unwanted contacts. By the use of such chaperones it is even possible for the cell to efficiently export and fold trimeric β-barrel structures such as porins, where the unfolded monomers are helped to assemble into trimers before membrane insertion [53,54].

Acknowledgements

D.K.D. and D.E.O. are supported by the Danish Research Foundation through inSPIN. S. Pedersen performed limited proteolysis experiments and T. Ebdrup cloned FkpA. We are very grateful to J. Kleinschmidt for supplying us with the expression vectors for Skp and to K.K. Andersen for help with refolding of wildtype OmpA.

References

[1] M. Karplus, D.L. Weaver, Prot. Sci. 3 (1994) 650–668.
[2] L.S. Itzhaki, D.E. Otzen, A.R. Fersht, J. Mol. Biol. 254 (1995) 260–288.
[3] G. de Prat-Gay, Protein Eng. 9 (1996) 843–847.
[4] M.L. Tasayco, J. Fuchs, X.M. Yang, D. Dyalram, R.E. Georgescu, Biochemistry 39 (2000) 10613–10618.
[5] M.L. Tasayco, J. Carey, Science 255 (1992) 594–597.
[6] K. Luger, U. Hommel, M. Herold, J. Hofsteenge, K. Kirschner, Science 243 (1989) 206–210.
[7] K. Luger, H. Szadkowski, K. Kirschner, Prot. Engin. 3 (1990) 249–258.
[8] G. de Prat Gay, A.R. Fersht, Biochemistry 33 (1994) 7957–7963.
[9] J. Ruiz-Sanz, G. de Prat Gay, D.E. Otzen, A.R. Fersht, Biochemistry 34 (1995) 1695–1701.
[10] J.L. Neira, L.S. Itzhaki, A.G. Ladurner, B. Davis, G. de Prat Gay, A.R. Fersht, J. Mol. Biol. 268 (1997) 185–197.
[11] M. Jourdan, M.S. Searle, Biochemistry 39 (2000) 12355–12364.
[12] J.L. Neira, B. Davis, A.G. Ladurner, A.M. Buckle, G. de Prat Gay, A.R. Fersht, Fold. Des. 1 (1996) 189–208.
[13] H.J. Dyson, J.R. Sayre, G. Merutka, H.C. Shin, R.A. Lerner, P.E. Wright, J. Mol. Biol. 226 (1992) 819–835.
[14] H.J. Dyson, G. Merutka, J.P. Waltho, R.A. Lerner, P.E. Wright, J. Mol. Biol. 226 (1992) 795–817.
[15] J.L. Popot, D.M. Engelman, Ann. Rev. Biochem. 69 (2000) 881–922.
[16] J.L. Popot, S.E. Gerchman, D.M. Engelman, J. Mol. Biol. 198 (1987) 655–676.
[17] S.H. White, W.C. Wimley, Ann. Rev. Biophys. Biomol. Struct. 28 (1999) 319–365.
[18] S.H. White, A.S. Ladokhin, S. Jayasinghe, K. Hristova, J. Biol. Chem. 276 (2001) 32395–32398.
[19] J.-L. Popot, D.M. Engelman, Biochemistry 29 (1990) 4031–4037.
[20] J.F. Hunt, T.N. Earnest, O. Bousché, K. Kalghatgi, K. Reilly, C. Horváth, K.J. Rothschild, D.M. Engelman, Biochemistry 36 (1997) 15156–15176.
[21] T. Hessa, H.J. Kim, K. Bihlmaler, C. Lundin, J. Boekel, H. Andersson, I.M. Nilsson, S.H. White, G. Von Heijne, Nature 433 (2005) 377–381.
[22] K.S. Huang, H. Bayley, M.J. Liao, E. London, H.G. Khorana, J. Biol. Chem. 256 (1981) 3802–3809.
[23] T. Marti, J. Biol. Chem. 273 (1998) 9312–9322.
[24] K.H. Zen, E. McKenna, E. Bibi, D. Hardy, H.R. Kaback, Biochemistry 33 (1994) 8198–8206.
[25] J.H. Kleinschmidt, T. den Blaauwen, A.J.M. Driessen, L.K. Tamm, Biochemistry 38 (1999) 5006–5016.
[26] J.H. Kleinschmidt, L.K. Tamm, J. Mol. Biol. 324 (2002) 319–330.
[27] E. Gouaux, J. Struct. Biol. 121 (1998) 110–122.
[28] N. Tobkes, B.A. Wallace, H. Bayley, Biochemistry 24 (1985) 1915–1920.
[29] J.M. Rausch, J.R. Marks, R. Rathinakumar, W.C. Wimley, Biochemistry 46 (2007) 12124–12139.
[30] L.K. Tamm, H. Hong, B. Liang, Biochim. Biophys. Acta 1666 (1–2) (2004) 250–263.
[31] R. De Mot, G. Schoofs, A. Roelandt, P. Declerck, P. Proost, J. Van Damme, J. Vanderleyden, Microbiology 140 (1994) 1377–1387.
[32] R. Koebnik, EMBO J. 15 (1996) 3529–3537.
[33] T. Surrey, F. Jähnig, Proc. Natl. Acad. Sci. U. S. A. 89 (1992) 7457–7461.
[34] J.H. Kleinschmidt, M.C. Wiener, L.K. Tamm, Prot. Sci. 8 (1999) 2065–2071.
[35] G. Ried, R. Koebnik, I. Hindennach, B. Mutschler, U. Henning, Mol. Gen. Genet. 243 (1994) 127–135.
[36] R. Koebnik, J. Bact. 181 (1999) 3688–3694.
[37] U.K. Laemmli, Nature 227 (1970) 680–685.
[38] R.M. Horton, H.D. Hunt, S.N. Ho, J.K. Pullen, L.R. Pease, Gene 77 (1989) 61–68.
[39] P.V. Bulieris, S. Behrens, O. Holst, J.H. Kleinschmidt, J. Biol. Chem. 278 (2003) 9092–9099.
[40] A. Pautsch, J. Vogt, K. Model, C. Siebold, G.E. Schulz, Proteins 34 (1999) 167–172.
[41] C. Tian, M.D. Karra, C.D. Ellis, J. Jacob, K. Oxenoid, F. Sönnichsen, C.R. Sanders, Methods Enzymol. 394 (2005) 321–334.
[42] H. Hong, L.K. Tamm, Proc. Natl. Acad. Sci. U. S. A. 101 (2004) 4065–4070.
[43] P. Carter, L. Abrahmsén, J.A. Wells, Biochemistry 30 (1991) 6142–6148.
[44] P. Carter, J.A. Wells, Science 1237 (1987) 394–399.
[45] J. Qu, S. Behrens-Kneip, O. Holst, J.H. Kleinschmidt, Biochemistry 48 (2009) 4926–4936.
[46] J.E. Mogensen, D.E. Otzen, Mol. Microbiol. 57 (2005) 326–346.
[47] R. Koebnik, L. Krämer, J. Mol. Biol. 250 (1995) 617–626.
[48] A.M. Fernandez-Escamilla, F. Rousseau, J. Schymkowitz, L. Serrano, Nat. Biotechnol. 22 (2004) 1302–1306.
[49] S.J. Allen, J.-M. Kim, H.G. Khorana, H. Lu, P.J. Booth, J. Mol. Biol. 308 (2001) 423–435.
[50] C.M. Bishop, W.F. Walkenhorst, W.C. Wimley, J. Mol. Biol. 309 (2001) 975–988.
[51] V. Visudtiphole, M.B. Thomas, D.A. Chalton, J.H. Lakey, Biochem J. 392 (2005) 375–381.
[52] D.E. Otzen, P.H. Nielsen, Cell. Mol. Life Sci. 65 (2008) 910–927.
[53] N. Harms, G. Koningstein, W. Dontje, M. Muller, B. Oudega, J. Luirink, H. de Cock, J. Biol. Chem. 276 (2001) 18804–18811.
[54] C. Jansen, M. Heutink, J. Tommassen, H. De Cock, Eur. J. Biochem. 267 (2000) 3792–3800.